ACS APPLIED MATERIALS & INTERFACES

Research Article

www.acsami.org

One-Step Process for High-Performance, Adhesive, Flexible Transparent Conductive Films Based on p-Type Reduced Graphene Oxides and Silver Nanowires

Yi-Ting Lai and Nyan-Hwa Tai*

Department of Materials Science and Engineering, National Tsing-Hua University, No. 101, Sec. 2, Kuang-Fu Road, Hsin-chu, 30013, Taiwan

Supporting Information

ABSTRACT: This work demonstrates a one-step process to synthesize uniformly dispersed hybrid nanomaterial containing silver nanowires (AgNWs) and p-type reduced graphene (p-rGO). The hybrid nanomaterial was coated onto a polyethylene terephthalate (PET) substrate for preparing high-performance flexible transparent conductive films (TCFs). The p-rGO plays the role of bridging discrete AgNWs, providing more electron holes and lowering the resistance of the contacted AgNWs; therefore, enhancing the electrical conductivity without sacrificing too much transparence of the TCFs. Additionally, the p-rGO also improves the adhesion between AgNWs and substrate by covering the AgNWs on the substrate tightly. The study shows that coating of the hybrid nanomaterials on the PET substrate demonstrates exceptional optoelectronic properties with a transmittance of 94.68% (at a wavelength of 550 nm) and a sheet resistance of 25.0 ± 0.8 Ω/sq. No significant variation in electric resistance can be detected even when the film was subjected to a bend loading with a radius of curvature of 5.0 mm or the film was loaded with a reciprocal tension or compression for 1000 cycles. Furthermore, both chemical corrosion resistance and haze effect were improved when p-rGO was introduced. The study shows that the fabricated flexible TCFs have the potential to replace indium tin oxide film in the optoelectronic industry.

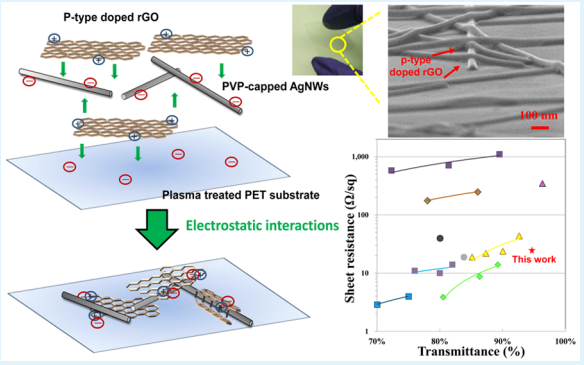

KEYWORDS: *silver nanowires, reduced graphene oxide, p-type doping, flexible transparent conductive films, one-step process*

INTRODUCTION

Recently, transparent conductive films (TCFs) have been widely used in optoelectronic devices such as organic light-emitting diodes, liquid crystal displays, touch panels, and solar cells. Indium tin oxide (ITO) is by far the most popular material adopted in TCFs.[1] However, ITO has many drawbacks such as brittleness, low adhesion to polymeric materials, a decrease in supply of indium, and the growing cost of indium metal, which have caused restrictions in its applications.[2,3] In addition, the ITO layer is usually fabricated in an expensive vacuum sputter system, resulting in a significant cost increases of the ITO-based products. Thus, there is an imperative demand in finding new materials to replace ITO in the fabrication of TCFs; in this regard, several materials including conductive polymers,[4] carbon nanotubes,[5,6] graphene,[7,8] and metal grids[9] have been proposed for the purpose. Among these alternatives, graphene can be a promising material for the substitution of ITO due to its superior mechanical flexibility and excellent optical transparency as well as outstanding thermal and electrical properties.[7,8]

Single layer graphene is usually synthesized by chemical vapor deposition (CVD) which has the advantages of controlled growth parameters and large area production. However, it inevitably requires a long processing time, high processing temperature up to 1000 °C, and low out-throughput, resulting in a high power consumption for mass production.[8,10] In addition, the CVD method requires an etching process to remove the metal substrate and a transferring process to fabricate flexible TCFs, resulting in ripples, wrinkles, folds, cracks and polymer residues, which degrade the electrical properties of the graphene.[10]

Reduced graphene oxide (rGO) is also an alternative material to fabricate TCFs. The solution-based processing for preparing graphene oxide (GO) possesses the characteristics of simple, exceptionally low cost, and large-scale or mass production.[11,12] However, the rGO converted from GO inevitably contains oxygen functional groups and lattice defects, which definitely degrade its electrical properties.[13] The reduction process usually produces nonuniform films due to difficulty in dispersing rGO in solution and favoring in restacking during reduction.[11,12,14] In addition, the reducing agents such as

Received: June 3, 2015
Accepted: August 6, 2015
Published: August 6, 2015

ACS Publications © 2015 American Chemical Society

DOI: 10.1021/acsami.5b04875
ACS Appl. Mater. Interfaces 2015, 7, 18553−18559

hydrazine might be highly toxic to humans and the environment.[12]

Recently, silver nanowires (AgNWs) have attracted increasing attention to TCFs due to its excellent electrical and optical properties which is arousing intensive interest in studying the feasibility of the AgNWs-based film to replace the ITO film.[15,16] Importantly, AgNWs can be uniformly dispersed in ink and printed on a large-scale substrate, which has exhibited excellent mechanical flexibility.[15,16] However, there are several serious challenging issues on the applications of optoelectronic devices. One of them is that the high resistance of the AgNW films arises at the network junctions of wires−wires. In addition, the films have large noncontacted areas in the partially percolated network, which result in high electrical resistance.[14,17] Furthermore, the poor adhesion between the AgNW films and the plastic substrates also restrict their applications into commercial devices.[17−19]

Preparation of AgNWs-related films for flexible TCFs have been proposed. In Chen's work,[20] the authors synthesized single-layer graphene and subsequently percolated with AgNWs to produce a conductive electrode on the PET substrate, which possessed an electrical resistivity of 22 ohm/sq and a transmittance of 88%. In Naito's work,[21] AgNWs and graphene were synthesized separately, which were then coated sequentially onto a transparent substrate; a conducted film with an electrical resistivity of 4 ohm/sq and a transmittance of 75% was reported. In Lee's work,[22] AgNWs were first synthesized onto a substrate which was subsequently deposited with graphene through the CVD method. The film with an electrical resistivity and a transmittance of 34.4 ohm/sq and 92.8%, respectively, was prepared.

In this study, we developed a facile and fast one-step process to prepare the AgNW/graphene slurry for the preparation of flexible TCFs. The process contained concurrent synthesis of AgNWs, reduction of GO, and formation of chloride-ion-doped graphene. The presence of doped graphene reduces the contact resistance and improves the connection between AgNWs;[23] furthermore, adhesion between AgNWs and substrate can also be enhanced and, as a result, significantly alleviates the reduction of electrical conductivity under bending.

EXPERIMENTAL SECTION

Materials. Silver nitrate ($AgNO_3$), ethylene glycol (EG), poly(vinylpyrrolidone) (PVP, MW ≈ 360 000) were purchased from Sigma-Aldrich. Potassium bromide (KBr) was purchased from Fluka, and sodium chloride (NaCl) was purchased from Showa. All chemicals were used without further purification. GO was synthesized from nature graphite powder (325 mesh, Alfa Aesar) through our previous work.[25]

One-Step Process for Preparing p-rGO/AgNW Slurry. A mixture of 0.3 g of PVP, 0.002 g of KBr, and 15 mL of EG was heated at 165 °C in an oil bath. Then 0.025 g of AgCl (synthesized by $AgNO_3$ and NaCl) dispersed in 5 mL of EG solution was added to the mixture slowly for obtaining Ag nucleation seeds. After 3 min, 0.11 g of $AgNO_3$ dissolved in 15 mL of EG solution was introduced slowly in 10 min for obtaining desirable nanowire configuration. After reaction for 2 h, 2 mg of GO dispersed in EG (1 mg/mL) was added to the mixture and thermally stabilized at 165 °C for another 48 h. The cooled-down solution was then precipitated with acetone and centrifuged at 1000 rpm for 5 min. Then, the supernatant containing the long/thin wires was washed three times with ethanol through centrifugation at 5000 rpm and dispersed into methanol (0.5 mg/mL) to obtain the hybrid nanomaterials of p-rGO/AgNWs.

Fabrication of Flexible TCFs. The PET films were first cleaned with ethanol and DI water and subsequently treated with O_2 plasma for 3 min to implant polar oxygen groups onto the PET surface, as a result, produced a PET film possessing high hydrophilicity. The presence of oxygen groups contributes an electrostatic interaction between the hydrophilic PET substrate and p-rGO, which enhance the adhesion between the coated film and PET substrate. The wire-wound coating method was utilized to fabricate the TCFs on the treated PET film.

Characterizations. Film morphologies of the samples were characterized by a field emission scanning electron microscope (FESEM, JEOL JSM-6500F) and a high-resolution transmission electron microscope (HRTEM, JEM 3000F). The thickness of the sample was measured by an atomic force microscope in tapping mode (Nanoscope IIIa, Digital Instruments Co.). The phase structures were verified using an X-ray diffraction (XRD 6000, Shimadzu). A Raman spectroscope (Horiba Jobin Yvon LABRAM HR 800 UV) equipped with a 632.8 nm He−Ne laser was used to characterize the nanostructures of EG, GO, and p-GO. The chemical states of the films were measured by an X-ray photoelectron spectroscopy (XPS, ESCA Ulvac-PHI PHI 1600). The sheet resistance was measured using a two-probe method where the probes were positioned at two different square copper contacts deposited on a TCF. The optical transmittance was measured using a UV−vis-NIR spectrophotometer (U-3010, Hitachi). The haze value was measured using a UV−vis spectrophotometer (Rainbow Light TSM-01).

RESULTS AND DISCUSSION

XRD analysis revealed that the dominant peak for the (002) plane at 26.5° is shifted to 9.6° after the graphite was oxidized to GO (see Figure 1), indicating that the interlayer distance of

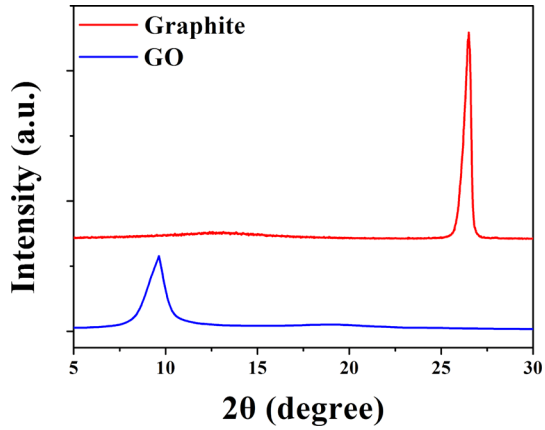

Figure 1. XRD patterns of graphite and GO; the graphitic peak (002) has shifted to a lower angle after oxidation, indicating the exfoliation of the graphite layer.

graphite layer increases from 0.34 to 0.92 nm. The increment of layer distance in GO is due to the presence of oxygen functional groups on the GO surface as well as the intercalation of oxygen functional groups between GO.[25]

When AgNWs were growing, the GO was slowly added into this solution and reduced to rGO by EG (EG has high reduction ability for GO at high temperature) to prepare the p-rGO/AgNWs hybrid nanomaterials. During the reduction process, the chloride ions were adsorbed onto the surface of graphene and react with the carbon atoms; in addition, halogenating preferentially occurs along the edges, where they are more energetically favorable. Because of chlorine possessing higher electronegativity than carbon, electrons on graphene are attracted by the chlorine, as a result, generating electron holes on the graphene which contributes to the p-type doped effect.[24,26] Besides, the PVP-coated AgNWs are known to be

DOI: 10.1021/acsami.5b04875
ACS Appl. Mater. Interfaces 2015, 7, 18553−18559

negatively charged;[27] therefore, through the new one-step process, the p-rGO can be dispersed uniformly in the hybrid system due to the electrostatic interactions with the AgNWs. FESEM was used to provide evidence for understanding morphologies of the hybrid films. Figure 2a shows that the

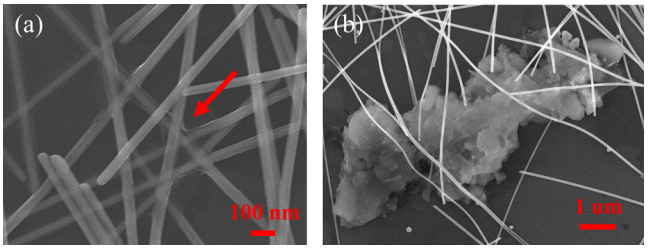

Figure 2. FESEM images of (a) the AgNWs network uniformly covered and wrapped by p-rGO as shown, indicating the well incorporation of the AgNWs and p-rGO via the one-step process; (b) aggregation of rGO causes the difficulty in coating process and affects the optoelectronic performances of TCFs.

AgNWs with the lengths of 10−20 um and the diameters of 40−70 nm are covered and wrapped by p-rGO (as depicted by the arrow in Figure 2a). In contrast, if the GO has been reduced in advance, it became difficult for the hybrid nanomaterials to be uniformly coated onto the substrates due to poor dispersity as well as aggregation of rGO in nature (Figure 2b). Dispersion of the hybrid nanomaterials without the p-type doped effect are observed in Figure S1, Supporting Information. Figure 3 is a

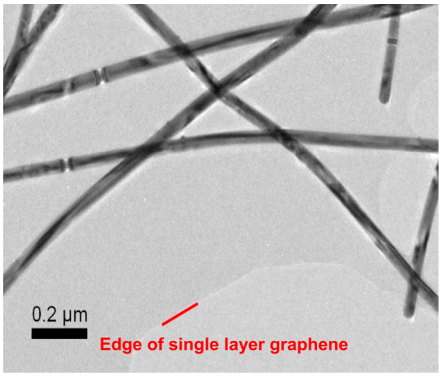

Figure 3. TEM image of the hybrid nanomaterial, indicating AgNWs are covered by large scale graphene.

TEM image of the hybrid nanomaterial. The red line is the edge of single layer graphene, which shows that the large-scale p-rGO can cover the AgNWs uniformly and provide more conductive pathways.

Raman spectroscopy was used to further understand the doping effect of chloride ions on graphene, as shown in Figure 4a, the prominent peaks at ∼1330 and ∼1580 cm^{-1} were assigned as D- and G-bands, respectively. The D-band is referred to the disordered sp^3 hybridized carbon as found in defects or impurities in carbon materials, while the G-band is resulting from the E2g vibrational mode of sp^2 bonded carbon.[10] The G-band in graphitic materials typically upshifts for electron-acceptor dopants and downshifts for electron-donor dopants.[28] Once the chloride ions were adsorbed onto the graphene surface, electrons on the graphitic framework are attracted toward the more electronegative chloride atoms, leading to G-band upshift. As shown in Figure 4a, the Raman spectrum G-band of the hybrid nanomaterials is over rGO shifting from 1583 to 1591 cm^{-1} (∼8 cm^{-1}).

XPS was used to characterize the chemical bonding of the hybrid film. In the wide XPS spectrum of the hybrid nanomaterials, as shown in Figure 4b, the peaks at ∼284.8 and ∼200.0 eV correspond to, respectively, C 1s of sp^2 hybridized carbon and Cl 2p of covalent bonds between carbon and chloride.[24,29] High-resolution C 1s and Cl 2p XPS spectra are shown in Figure 4c,d, suggesting that the Cl atoms have doping interaction with graphene. The low intensity of functional groups present in the C 1s peak confirms the successful reduction of GO.[29] The Cl 2p spectrum shows two peaks separated by ∼1.6 eV, Cl 2p3/2, and Cl 2p1/2, which resulting from spin−orbit coupling.[24] The peak at ∼200.5 and ∼198.3 eV are assigned as C−Cl covalent bondings and $C-Cl^-$ ionic bondings, respectively.

Bending tests to study the flexibility of the hybrid TCFs were performed. Figure 5a shows the electrical sheet resistance and the variation in relative electrical sheet resistance as a function of radius of curvature. The relative electrical sheet resistance is defined as $(Rs - R_0)/R_0$, where Rs and R_0 are the electrical sheet resistances of the TCFs with or without subjecting bending, respectively. No significant increase in sheet resistance of the hybrid TCF was detected as the sample was bent to a radius of 4.5 mm. Even though the radius of curvature was further decreased to 0.2 mm, the sheet resistance of the hybrid TCF only slightly increased from 25.0 ± 0.8 to 28.0 ± 1.5 Ω/sq, indicating the outstanding flexibility of the hybrid films as compared with ITO.[2,3]

The electromechanical stabilities of the hybrid TCFs and the AgNW films as a function of bending cycles are compared in Figure 5b. The films on PET substrates were bent to a radius of curvature of 7.5 mm. The sheet resistances of the hybrid film on PET substrate subjected to compressive and tensile bending stresses were individually tested. In addition, the sheet resistances of the hybrid film subjected to tension and compression are 44.3 ± 0.8 and 32.2 ± 0.4 Ω/sq, respectively. All the films showed nearly constant sheet resistance within the initial 100 cycles. The sheet resistance of the AgNW film increase slowly in the subsequent tests; on the other hand, the sheet resistance of the hybrid film remained unchanged during the first 300 cycles and slightly increased but no higher than 5% after 1000 bending cycles. The results indicate that the electromechanical stability of the TCFs is improved due to the presence of p-rGO. The stabilities of chemical corrosion of hybrid and AgNW TCFs were depicted in Figure 6. In the test, the hybrid dispersion and AgNW were coated on PET substrates followed by immersion in water, ethanol, or acetone for 24 h or exposure to H_2S gas for 10 min. The sheet resistance of the hybrid film showed almost no change after immersion in water, ethanol, and acetone for 24 h; on the other hand, 1.1, 1.4, and 1.6-fold increase in sheet resistance of the AgNW films after immersion in water, ethanol, and acetone, respectively, were detected. In addition, the hybrid TCFs showed 1.5-fold increase after exposure in H_2S for 10 min indicating that the hybrid film possessed excellent corrosion resistance because uniform coating of p-rGO on AgNWs could prevent exposure of AgNWs from H_2S. In contrast, the AgNW film was oxidized quickly and the sheet resistance showed a 16.75-fold increase when exposed to H_2S for 10 min. The results indicate that the hybrid TCFs have prominent stability due to the presence of a p-rGO layer.

DOI: 10.1021/acsami.5b04875
ACS Appl. Mater. Interfaces 2015, 7, 18553−18559

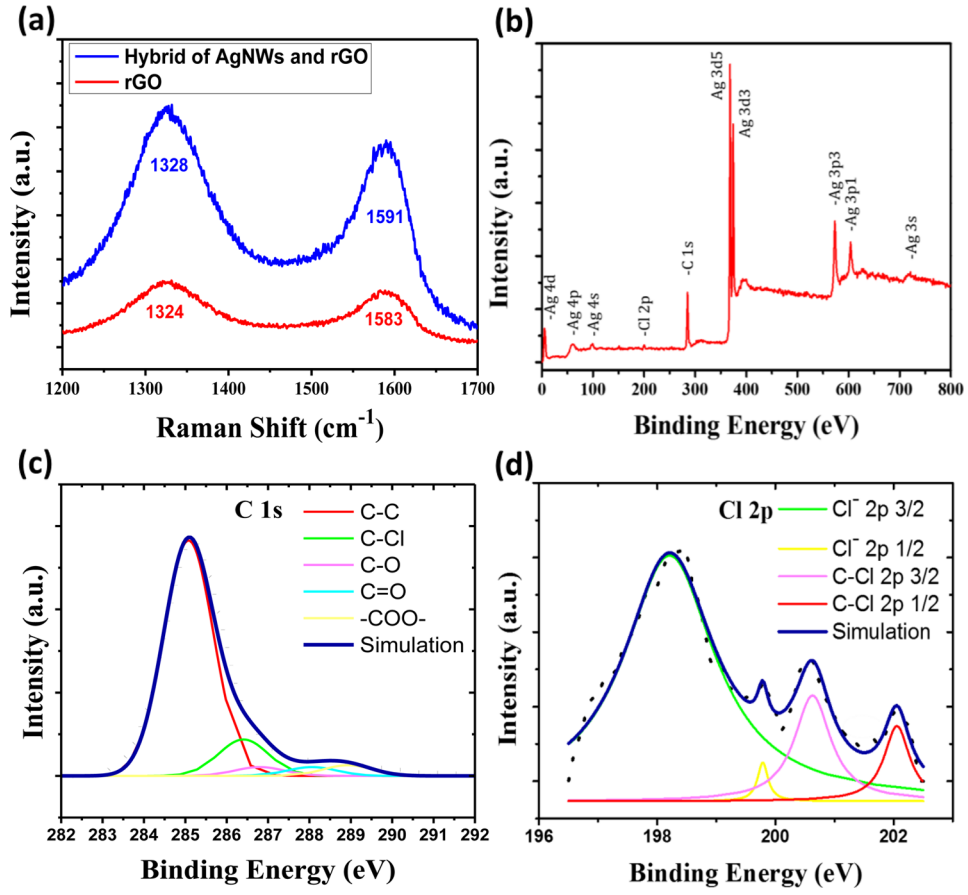

Figure 4. (a) Raman spectrum G-band of hybrid film is observed upshifted by ~6 cm^{-1} compared with pristine rGO. (b) XPS spectrum of the hybrid film. High-resolution of the (c) C 1s and (d) Cl 2p XPS spectra.

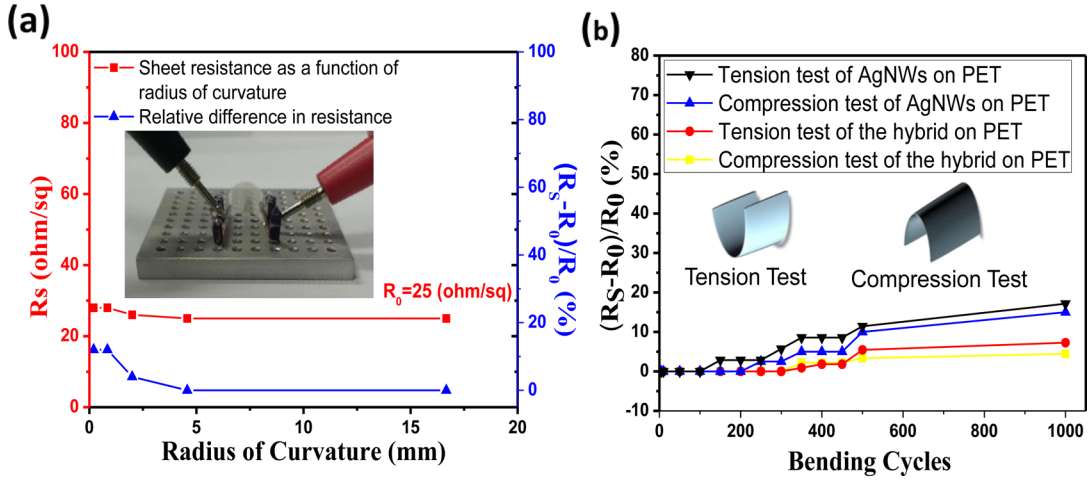

Figure 5. (a) Sheet resistance and relative difference in resistance as a function of the radius of curvature. (b) Variation of sheet resistance of the hybrid and AgNW films on the PET substrate as a function of bending cycles. The films were bent to the radius of curvature of 7.5 mm.

The adhesion of the hybrid TCFs is significantly improved through the electrostatic interaction among the p-rGO, AgNWs, and O_2 plasma treated PET. The FESEM image of the surface morphology of the hybrid film shows that the AgNWs are stacked against each other and tightly adhered to the substrate, in which the AgNWs are covered with p-rGO (as depicted by the arrows in Figure 7a). Adherence tests were performed using a 3 M Scotch tape, as shown in Figure 7b, and the FESEM image depicted that the p-rGO covers the AgNWs and protects them from detaching during the tape test. Therefore, majority of the AgNWs in the hybrid film could still adhere to the PET substrate, while the AgNWs film (without p-rGO covering) was completely detached by the tape (Figure S2, Supporting Information).

The mechanisms for the enhancement of the adhesion and conductivity of the hybrid TCFs are schematically illustrated in Figure 8. The p-rGO adhere tightly to the hydrophilic PET surfaces and negatively charged AgNWs owing to the

DOI: 10.1021/acsami.5b04875
ACS Appl. Mater. Interfaces 2015, 7, 18553−18559

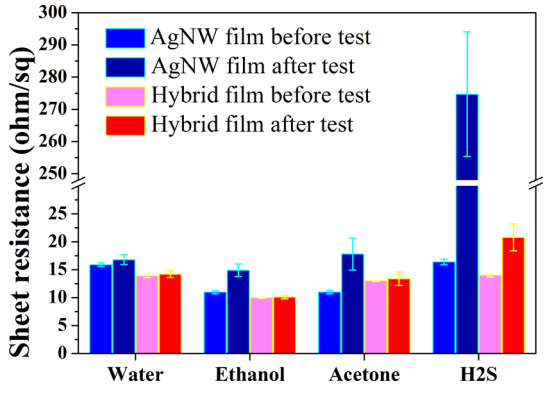

Figure 6. Changes of sheet resistance of hybrid films and AgNW films after separate exposure to water, ethanol, and acetone for 24 h and H_2S gas for 10 min.

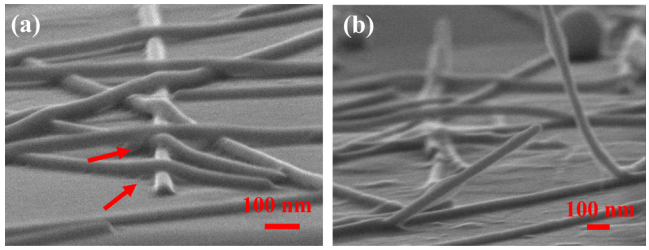

Figure 7. FESEM images of the hybrid film on PET substrate (a) before and (b) after the tape test.

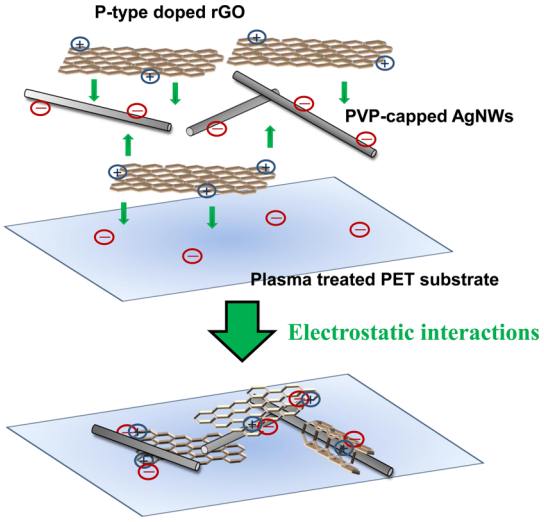

Figure 8. Schematic illustration the incorporation of the AgNWs and the p-rGO for preparing hybrid TCFs shown enhanced conductivity through the electrostatic interactions. In the film, p-rGO bridges the discrete AgNWs, which provide more conductive pathways through the defects and grain boundaries of p-rGO.

electrostatic interactions.[30] Figure 9a depicted that the contact area is relatively small without p-rGO, while the contact area was increased and AgNWs performed more comfortably when p-rGO was introduced, as shown in Figure 9b. The contact area of AgNWs is effectively increased and the adhesion is enhanced due to the presence of the p-rGO, leading to the decrease of junction resistance between AgNWs. The p-rGO can also bridge the discrete AgNWs and cover the void space formed by the entangled AgNWs, as indicated by the red arrows in Figure 7a, as a result, providing more conductive pathways for electron

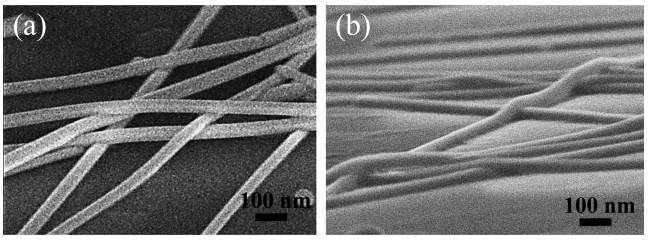

Figure 9. FESEM images of (a) pristine AgNWs film and (b) hybrid nanomaterials films.

transfer. Moreover, AgNWs can function as conductive bridges through the defects and grain boundaries of graphene. In addition, the p-type doped behavior of rGO cannot only increase the hole carriers but also improve the uniformity of TCFs by reducing the aggregation of rGO.[24] Although the mechanical pressing and the heating methods to improve the conductivity of AgNWs films have been reported,[14,21,23] the methods are not appropriate for fragile and low-melting point substrates. As compared with the published data shown in Figure 10,[6,8,12,20−22,31−33] this study demonstrated an one-step

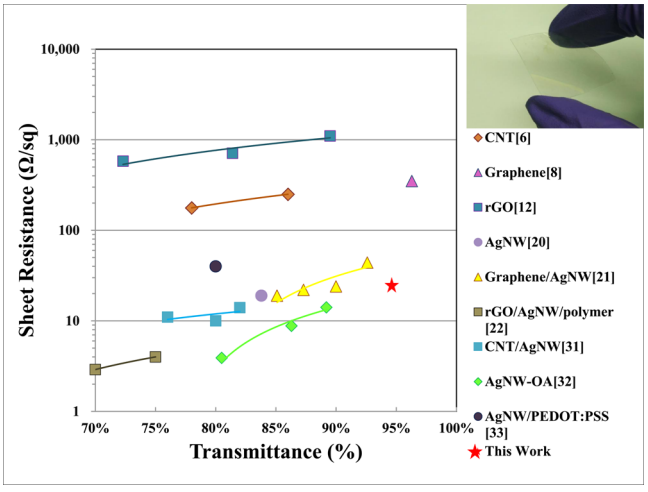

Figure 10. Transmittance values versus sheet resistance of previous studies and this work (the AgNWs/p-rGO hybrid film). The transmittance data of refs 22, 32, and 33 include the values of substrates, which are polymer, PET, and PET, respectively. The upper right inset image shows a flexible hybrid TCF on a PET substrate.[6,8,12,20−22,31−33]

process for preparing high-performance flexible TCFs which show exceptional optoelectronic properties with a transmittance of 94.68% (at a wavelength of 550 nm) and a sheet resistance of 25.0 ± 0.8 Ω/sq.

Thickness of the hybrid film was measured using atomic force microscopy, and the image shown in Figure 11a illustrates that the thickness of the p-rGO layer is approximate 1.29 nm. Figure 11b shows the transmittance and reflection spectra of the AgNW film and hybrid film. Although the transmittances of AgNW film and hybrid film are similar (~91% at 550 nm), the AgNW film possesses a mean reflectance of ~8.36%, while the hybrid film exhibits low haze effect with a mean reflectance of ~4.25% (the mean reflectance of PET substrate is ~2.26%). The haze effect may cause by the uniformity of the film.[34] The results indicate that the uniform coating of p-rGO can decrease

DOI: 10.1021/acsami.5b04875
ACS Appl. Mater. Interfaces 2015, 7, 18553−18559

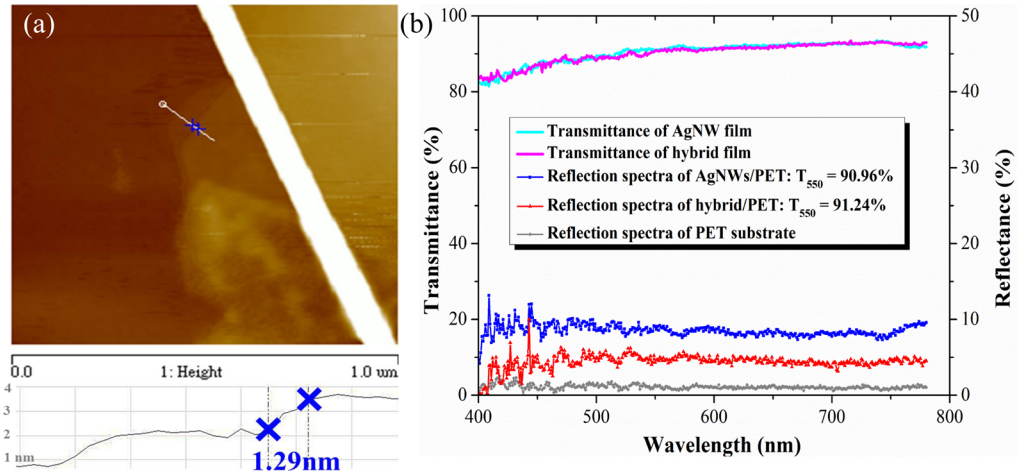

Figure 11. (a) AFM height images of hybrid materials. The plot beneath the topography is the height data of the hybrid film indicated by a white line in the AFM height image. (b) Optical transmittance ($T \sim 91\%$ at 550 nm) and reflection spectra of AgNWs/PET, hybrid/PET, and PET substrate in the visible light range.

the effect of light scattering, achieving the preparation of highly transparent and low-haze TCFs.

CONCLUSIONS

In conclusion, this study demonstrated the preparation of superiorly conductive, extremely transparent, and highly flexible hybrid TCFs via a facile and fast one-step process. The process can not only synthesize AgNWs, reduce and dope graphene oxide collaboratively, but also prevent the aggregation of p-rGO, leading to highly dispersible AgNWs and p-rGO in the hybrid TCF film. The presence of p-rGO plays the role of providing more electrical conductive pathways between non-contacted AgNWs and increasing the contact area of AgNWs. Moreover, the doping effect of rGO increases the hole carriers and results in strong electrostatic interactions between p-rGO, AgNWs, and O_2 plasma-treated PET substrates. Resistance to chemical corrosion of the hybrid films can also be enhanced because the p-rGO can prevent exposure of AgNWs from the oxidant. The electrostatic interactions can enhance the adhesion of AgNWs on the substrates, achieving the preparation of highly bendable and uniform TCFs with a transmittance of 94.68% and a sheet resistance of 25.0 ± 0.8 Ω/sq. Additionally, the hybrid film prepared through the facile process possesses very low haze effect with a mean reflectance of ~4.25%. The processing was completed using economical and all-solution processes, indicating the proposed methods can be applied to commercial applications in producing large-area TCFs for optoelectronic devices.

ASSOCIATED CONTENT

Supporting Information

The Supporting Information is available free of charge on the ACS Publications website at DOI: 10.1021/acsami.5b04875.

Additional experimental data, spectra, and images (PDF)

AUTHOR INFORMATION

Corresponding Author

*Phone: +886 35715131 ext. 42568. Fax: + 886 3 5737406. E-mail: nhtai@mx.nthu.edu.tw.

Notes

The authors declare no competing financial interest.

ACKNOWLEDGMENTS

The authors thank the support from National Science Council, Taiwan under the Contract 101-2221-E-007-064-MY3.

REFERENCES

(1) Tseng, S. F.; Hsiao, W. T.; Huang, K. C.; Chiang, D.; Chen, M. F.; Chou, C. P. Laser Scribing of Indium Tin Oxide (ITO) Thin Films Deposited on Various Substrates for Touch Panels. *Appl. Surf. Sci.* **2010**, *257*, 1487−1494.

(2) Cairns, D. R.; Witte, R. P.; Sparacin, D. K.; Sachsman, S. M.; Paine, D. C.; Crawford, G. P.; Newton, R. R. Strain-Dependent Electrical Resistance of Tin-Doped Indium Oxide on Polymer Substrates. *Appl. Phys. Lett.* **2000**, *76*, 1425−1427.

(3) Leterrier, Y.; Médico, L.; Demarco, F.; Månson, J. A. E.; Betz, U.; Escolà, M. F.; Kharrazi Olsson, M.; Atamny, F. Mechanical Integrity of Transparent Conductive Oxide Films for Flexible Polymer-Based Displays. *Thin Solid Films* **2004**, *460*, 156−166.

(4) Burroughes, J. H.; Bradley, D. D. C.; Brown, A. R.; Marks, R. N.; Mackay, K.; Friend, R. H.; Burns, P. L.; Holmes, A. B. Light-Emitting Diodes Based on Conjugated Polymers. *Nature* **1990**, *347*, 539−541.

(5) Tsai, T. Y.; Lee, C. Y.; Tai, N. H.; Tuan, W. H. Transfer of Patterned Vertically Aligned Carbon Nanotubes onto Plastic Substrates for Flexible Electronics and Field Emission Devices. *Appl. Phys. Lett.* **2009**, *95*, 013107.

(6) Abdelhalim, A.; Abdellah, A.; Scarpa, G.; Lugli, P. Fabrication of Carbon Nanotube Thin Films on Flexible Substrates by Spray Deposition and Transfer Printing. *Carbon* **2013**, *61*, 72−79.

(7) Nguyen, D. D.; Tai, N. H.; Chueh, Y. L.; Chen, S. Y.; Chen, Y. J.; Kuo, W. S.; Chou, T. W.; Hsu, C. S.; Chen, L. J. Synthesis of Ethanol-Soluble Few-Layer Graphene Nanosheets for Flexible and Transparent Conducting Composite Films. *Nanotechnology* **2011**, *22*, 295606.

(8) Gao, L.; Ren, W.; Zhao, J.; Ma, L. P.; Chen, Z.; Cheng, H. M. Efficient Growth of High-Quality Graphene Films on Cu Foils by Ambient Pressure Chemical Vapor Deposition. *Appl. Phys. Lett.* **2010**, *97*, 183109.

(9) Hu, L.; Wu, H.; Cui, Y. Metal Nanogrids, Nanowires, and Nanofibers for Transparent Electrodes. *MRS Bull.* **2011**, *36*, 760−765.

(10) Nguyen, D. D.; Tai, N.-H.; Chen, S. Y.; Chueh, Y.-L. Controlled Growth of Carbon Nanotube-Graphene Hybrid Materials for Flexible and Transparent Conductors and Electron Field Emitters. *Nanoscale* **2012**, *4*, 632−638.

(11) Nekahi, A.; Marashi, P. H.; Haghshenas, D. Transparent Conductive Thin Film of Ultra Large Reduced Graphene Oxide Monolayers. *Appl. Surf. Sci.* **2014**, *295*, 59−65.

(12) Karthick, R.; Brindha, M.; Selvaraj, M.; Ramu, S. Stable Colloidal Dispersion of Functionalized Reduced Graphene Oxide in

DOI: 10.1021/acsami.5b04875
ACS Appl. Mater. Interfaces 2015, 7, 18553−18559

Aqueous Medium for Transparent Conductive Film. *J. Colloid Interface Sci.* **2013**, *406*, 69−74.
(13) Feng, H.; Cheng, R.; Zhao, X.; Duan, X.; Li, J. A Low-Temperature Method to Produce Highly Reduced Graphene Oxide. *Nat. Commun.* **2013**, *4*, 1539.
(14) Liu, B. T.; Kuo, H. L. Graphene/Silver Nanowire Sandwich Structures for Transparent Conductive Films. *Carbon* **2013**, *63*, 390−396.
(15) De, S.; Higgins, T. M.; Lyons, P. E.; Doherty, E. M.; Nirmalraj, P. N.; Blau, W. J.; Boland, J. J.; Coleman, J. N. Silver Nanowire Networks as Flexible, Transparent, Conducting Films: Extremely High DC to Optical Conductivity Ratios. *ACS Nano* **2009**, *3*, 1767−1774.
(16) Hu, L.; Kim, H. S.; Lee, J. Y.; Peumans, P.; Cui, Y. Scalable Coating and Properties of Transparent, Flexible, Silver Nanowire Electrodes. *ACS Nano* **2010**, *4*, 2955−2963.
(17) Lee, M. S.; Lee, K.; Kim, S. Y.; Lee, H.; Park, J.; Choi, K. H.; Kim, H. K.; Kim, D. G.; Lee, D. Y.; Nam, S.; Park, J. U. High-Performance, Transparent, and Stretchable Electrodes Using Graphene−Metal Nanowire Hybrid Structures. *Nano Lett.* **2013**, *13*, 2814−2821.
(18) Ahn, Y.; Jeong, Y.; Lee, Y. Improved Thermal Oxidation Stability of Solution-Processable Silver Nanowire Transparent Electrode by Reduced Graphene Oxide. *ACS Appl. Mater. Interfaces* **2012**, *4*, 6410−6414.
(19) Choi, D. Y.; Kang, H. W.; Sung, H. J.; Kim, S. S. Annealing-Free, Flexible Silver Nanowire-Polymer Composite Electrodes *via* a Continuous Two-Step Spray-Coating Method. *Nanoscale* **2013**, *5*, 977−983.
(20) Jiu, J.; Nogi, M.; Sugahara, T.; Tokuno, T.; Araki, T.; Komoda, N.; Suganuma, K.; Uchida, H.; Shinozaki, K. Strongly Adhesive and Flexible Transparent Silver Nanowire Conductive Films Fabricated with a High-Intensity Pulsed Light Technique. *J. Mater. Chem.* **2012**, *22*, 23561−23567.
(21) Chen, R.; Das, S. R.; Jeong, C.; Khan, M. R.; Janes, D. B.; Alam, M. A. Co-Percolating Graphene-Wrapped Silver Nanowire Network for High Performance, Highly Stable, Transparent Conducting Electrodes. *Adv. Funct. Mater.* **2013**, *23*, 5150−5158.
(22) Naito, K.; Yoshinaga, N.; Tsutsumi, E.; Akasaka, Y. Transparent Conducting Film Composed of Graphene and Silver Nanowire Stacked Layers. *Synth. Met.* **2013**, *175*, 42−46.
(23) Lee, D.; Lee, H.; Ahn, Y.; Jeong, Y.; Lee, D.-Y.; Lee, Y. Highly Stable and Flexible Silver Nanowire-Graphene Hybrid Transparent Conducting Electrodes for Emerging Optoelectronic Devices. *Nanoscale* **2013**, *5*, 7750−7755.
(24) Wassei, J. K.; Cha, K. C.; Tung, V. C.; Yang, Y.; Kaner, R. B. The Effects of Thionyl Chloride on the Properties of Graphene and Graphene-Carbon Nanotube Composites. *J. Mater. Chem.* **2011**, *21*, 3391−3396.
(25) Nguyen, D. D.; Lai, Y. T.; Tai, N. H. Enhanced Field Emission Properties of a Reduced Graphene Oxide/Carbon Nanotube Hybrid Film. *Diamond Relat. Mater.* **2014**, *47*, 1−6.
(26) Parekh, B. B.; Fanchini, G.; Eda, G.; Chhowalla, M. Improved Conductivity of Transparent Single-Wall Carbon Nanotube Thin Films *via* Stable Postdeposition Functionalization. *Appl. Phys. Lett.* **2007**, *90*, 121913.
(27) Luu, Q. N.; Doorn, J. M.; Berry, M. T.; Jiang, C.; Lin, C.; May, P. S. Preparation and Optical Properties of Silver Nanowires and Silver-Nanowire Thin Films. *J. Colloid Interface Sci.* **2011**, *356*, 151−158.
(28) Rao, A. M.; Eklund, P. C.; Bandow, S.; Thess, A.; Smalley, R. E. Evidence for Charge Transfer in Doped Carbon Nanotube Bundles from Raman Scattering. *Nature* **1997**, *388*, 257−259.
(29) Jo, K.; Lee, T.; Choi, H. J.; Park, J. H.; Lee, D. J.; Lee, D. W.; Kim, B.-S. Stable Aqueous Dispersion of Reduced Graphene Nanosheets *via* Non-Covalent Functionalization with Conducting Polymers and Application in Transparent Electrodes. *Langmuir* **2011**, *27*, 2014−2018.
(30) Li, Y.; Cui, P.; Wang, L.; Lee, H.; Lee, K.; Lee, H. Highly Bendable, Conductive, and Transparent Film by an Enhanced Adhesion of Silver Nanowires. *ACS Appl. Mater. Interfaces* **2013**, *5*, 9155−9160.
(31) Stapleton, A. J.; Afre, R. A.; Ellis, A. V.; Shapter, J. G.; Andersson, G. G.; Quinton, J. S.; Lewis, D. A. Highly Conductive Interwoven Carbon Nanotube and Silver Nanowire Transparent Electrodes. *Sci. Technol. Adv. Mater.* **2013**, *14*, 035004.
(32) Miller, M. S.; O'Kane, J. C.; Niec, A.; Carmichael, R. S.; Carmichael, T. B. Silver Nanowire/Optical Adhesive Coatings as Transparent Electrodes for Flexible Electronics. *ACS Appl. Mater. Interfaces* **2013**, *5*, 10165−10172.
(33) Wu, L. Y. L.; Kerk, W. T.; Wong, C. C. Transparent Conductive Film by Large Area Roll-to-Roll Processing. *Thin Solid Films* **2013**, *544*, 427−432.
(34) Szanyi, J. The Origin of Haze in CVD Tin Oxide Thin Films. *Appl. Surf. Sci.* **2002**, *185*, 161−171.

DOI: 10.1021/acsami.5b04875
ACS Appl. Mater. Interfaces 2015, 7, 18553−18559